

Intrinsic Electron Accumulation at Clean InN Surfaces

I. Mahboob, T. D. Veal, and C. F. McConville*

Department of Physics, University of Warwick, Coventry, CV4 7AL, United Kingdom

H. Lu and W. J. Schaff

Department of Electrical and Computer Engineering, Cornell University, Ithaca, New York 14853, USA

(Received 8 September 2003; published 22 January 2004)

The electronic structure of clean InN(0001) surfaces has been investigated by high-resolution electron-energy-loss spectroscopy of the conduction band electron plasmon excitations. An intrinsic surface electron accumulation layer is found to exist and is explained in terms of a particularly low Γ -point conduction band minimum in wurtzite InN. As a result, surface Fermi level pinning high in the conduction band in the vicinity of the Γ point, but near the average midgap energy, produces charged donor-type surface states with associated downward band bending. Semiclassical dielectric theory simulations of the energy-loss spectra and charge-profile calculations indicate a surface state density of $2.5 (\pm 0.2) \times 10^{13} \text{ cm}^{-2}$ and a surface Fermi level of $1.64 \pm 0.10 \text{ eV}$ above the valence band maximum.

DOI: 10.1103/PhysRevLett.92.036804

PACS numbers: 73.20.At, 73.20.Mf, 79.20.Kz

Recently, InN has attracted much attention because of the revision of the fundamental band gap energy from 1.8–2.1 to 0.7–0.8 eV [1]. Consequently, the band gap of the ternary alloy InGaN is now known to span from the near infrared of InN to the ultraviolet of GaN, thus enabling the entire optical window to be encompassed by a single material system [2]. In order to fully realize the potential of InN, a fundamental understanding of the surface and interface properties is required, since these will have a major influence on the design criteria of low dimensional devices. There has been some evidence to suggest the presence of electron accumulation at the surface of InN, including measurements of the sheet carrier density as a function of InN film thickness and capacitance-voltage profiling [3]. Photoemission results from Ti deposited on Ar-sputtered InN also indicate the existence of an electron accumulation layer [4]. Crucially, since all of these techniques required either metal deposition or the formation of contacts to the InN surface, they cannot be used to characterize the free surface. As a result, it is not clear whether an intrinsic electron accumulation layer is present at clean InN surfaces. In this Letter, a high-resolution electron-energy-loss spectroscopy (HREELS) investigation reveals the existence of intrinsic electron accumulation at clean InN surfaces by removing the need to form contacts [5–7].

The InN(0001) samples used in this study were grown with unintentional n -type doping by migration enhanced gas source molecular beam epitaxy on a sapphire substrate with an AlN buffer layer. Details of the growth can be found elsewhere [8]. Following insertion into the HREELS vacuum chamber, InN surface preparation was achieved *in situ* by atomic hydrogen cleaning (AHC) [9]. A two-stage AHC process was used consisting of two 10 kL doses of H_2 , the first at room temperature and the second at 600 K. This surface preparation resulted in a

(1×1) reconstruction as indicated by low-energy electron diffraction. HREELS confirmed the removal of atmospheric contaminants by the absence of vibrational modes associated with adsorbed hydrocarbons and native oxides. The conduction band plasmon excitations are probed using HREELS to measure the plasma frequency-depth profile. A monoenergetic beam of low-energy electrons couple to the electric fields of the surface plasmons arising from the free carriers in the conduction band, resulting in electron-energy-loss spectra. By varying the energy of the probing electrons, the entire space-charge region (up to 200 Å) can be surveyed [5,6].

A series of normalized HREEL spectra recorded from the clean InN(0001) surface with a range of probing energies is shown in Fig. 1, along with semiclassical dielectric theory simulations. Two distinct features are observed in the HREEL spectra. The first loss feature at $\sim 66 \text{ meV}$ is assigned to Fuchs-Kliewer surface phonon excitations [10]. The reduction in phonon peak intensity as the probing electron energy is increased is due to the phonon polarization field being screened by the conduction electrons. The second loss feature at $\sim 250 \text{ meV}$ is due to conduction band electron plasmon excitations. The plasmon peak undergoes a $\sim 30 \text{ meV}$ downward dispersion as the energy of the probing electrons is increased from 10 to 30 eV. This can be understood in terms of a surface layer of higher plasma frequency than that of the bulk and provides direct evidence for the existence of an electron accumulation layer at the InN surface. Additionally, the width of the plasmon feature is due to a rapidly varying plasma frequency profile. As a result, no single plasma frequency dominates, which is consistent with an accumulation layer plasma frequency profile.

In order to quantify the surface space-charge properties of InN, the HREEL spectra were simulated using a wave vector-dependent dielectric function [5,11]. A

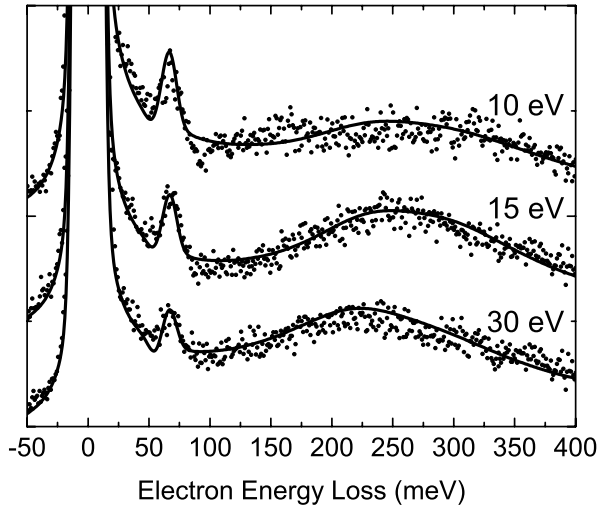


FIG. 1. Specular HREEL spectra recorded at 300 K from an atomic hydrogen cleaned InN(0001)-(1 × 1) surface with incident electron energies of 10, 15, and 30 eV (points) and the corresponding semiclassical dielectric theory simulations (solid lines).

four-layer model was required to simulate the HREEL spectra, the individual layer properties of which are summarized in Table I. A plasma dead layer of 3 Å was required, to both simulate the variation in the phonon intensity and approximate the quantum mechanical effect of the surface potential barrier. Two further layers of enhanced plasma frequency were also needed to reproduce the plasmon tail at high loss energy. Finally, a bulk layer with a plasma frequency ω_p of 211 meV reproduced the plasmon peak position. This layer profile was necessary to reproduce the dispersion of the plasmon peak. The results of the HREELS simulations are shown in Fig. 1, where all the spectra were simulated using the same plasma frequency profile.

Figure 2 shows the variation of plasma frequency and electron effective mass at the Fermi level as a function of the conduction electron concentration. In these calculations, a band gap E_g of 0.75 eV [1] was used, with an electron effective mass at the conduction band minimum

TABLE I. The plasma frequency profile used in the dielectric theory simulations of the HREEL spectra and the corresponding electronic properties. These carrier statistics were calculated from the conduction band dispersion relation modeled by a two-band $\mathbf{k} \cdot \mathbf{p}$ band structure that incorporates electron-electron interactions and electron-ionized impurity interactions in the high wave vector regime.

Layer	1	2	3	4
d (Å)	3 ± 0.5	6 ± 0.5	30 ± 1	∞
ω_p (meV)	0	422 ± 13	282 ± 2.5	211 ± 1.5
n (10^{20} cm^{-3})	0	2.84	0.77	0.32
m_F^*/m_0	...	0.33	0.20	0.15

m_0^* of 0.07 [12] and a high frequency dielectric constant $\epsilon(\infty)$ of 6.7 [13]. A two-band $\mathbf{k} \cdot \mathbf{p}$ band structure model was utilized to calculate the nonparabolic dispersion of the conduction band [14]. This model was modified for application in the large wave vector and high Fermi level regime by incorporating electron-electron interactions and electron-ionized impurity interactions [12,15]. The resulting conduction band dispersion relation enabled the calculation of the semiconductor statistics that is the plasma frequency and the electron effective mass at the Fermi level as a function of electron concentration, as detailed in Ref. [16] and shown in Fig. 2. These calculations were used to translate the plasma frequencies extracted from the HREELS simulations into carrier concentrations. The resulting conduction electron-depth profile, determined from the HREELS simulations for InN, is presented in Fig. 3 and summarized in Table I. A maximum electron density of $\sim 2.8 \times 10^{20} \text{ cm}^{-3}$ occurs in the near surface, declining to the bulk carrier concentration of $3.2 \times 10^{19} \text{ cm}^{-3}$. This analysis clearly confirms the presence of an intrinsic electron accumulation layer on the clean InN surface.

Realistic smooth charge profiles were calculated to determine the surface state density, the band bending, and the position of the Fermi level at the surface. The smooth charge profile that most closely resembles the HREELS simulation profile is shown in Fig. 3, along with the corresponding potential profile. The charge profiles were calculated by solving the Poisson equation within the modified Thomas-Fermi approximation (MTFA). The carrier concentration as a function of depth

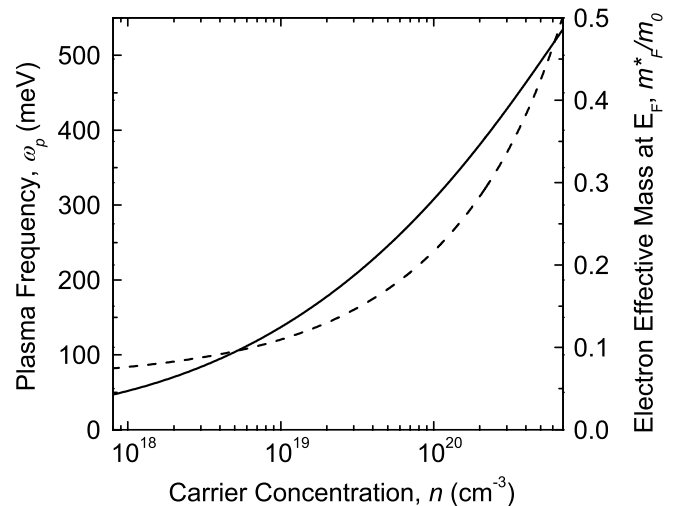


FIG. 2. The plasma frequency (solid line) and the electron effective mass at the Fermi level (dashed line) calculated as a function of the carrier concentration for InN. These carrier statistics were calculated from the conduction band dispersion relation modeled by a two-band $\mathbf{k} \cdot \mathbf{p}$ band structure that incorporates electron-electron interactions and electron-ionized impurity interactions in the high wave vector regime.

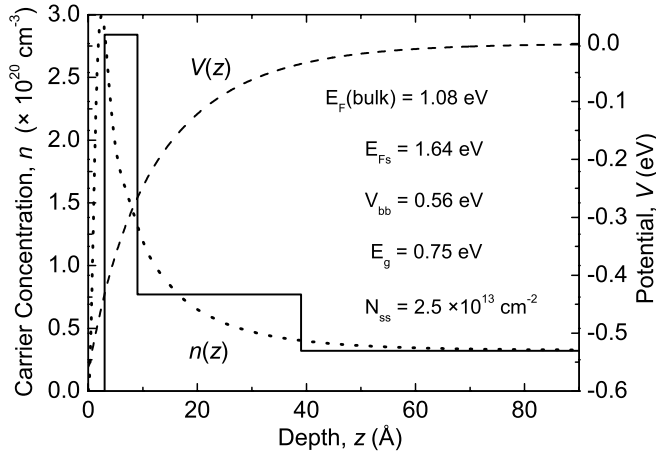


FIG. 3. The layered charge profile used in the HREELS simulations (solid line) and the corresponding smooth charge profile $n(z)$ calculated by solving the Poisson equation within the MTF (dotted line). Also shown is the potential profile $V(z)$ (dashed line). The bulk and surface Fermi level values are referenced to the valence band maximum.

$n(z)$ depends on the local Fermi level, which is determined by the bulk Fermi level and the value of the potential $V(z)$, which, in turn, is given by the solution to the Poisson equation [17]. The MTF takes account of the quantized nature of the electron wave functions, whereby the surface potential barrier reduces the carrier density to zero at the surface. Importantly, solving the Poisson equation within the MTF also allows the conduction band nonparabolicity to be incorporated straightforwardly without requiring full self-consistent solutions of the Schrödinger and Poisson equations [18]. This charge-profile calculation yields a surface state density N_{ss} of $\sim(2.5 \pm 0.2) \times 10^{13} \text{ cm}^{-2}$, giving rise to an electric field of $4.7 \times 10^8 \text{ V m}^{-1}$ at the surface and band bending V_{bb} of $\sim 0.56 \text{ eV}$. As a result of this band bending, the surface Fermi level E_{Fs} is located $\sim 1.64 \pm 0.10 \text{ eV}$ above the valence band maximum (VBM). The uncertainties given for the values of surface state density and surface Fermi level include both the uncertainty in determining the plasma frequency profile from the dielectric theory simulations and the uncertainty introduced by the band gap of InN being known only to within the range 0.7–0.8 eV. The values reported for N_{ss} and E_{Fs} are for a band gap of 0.75 eV.

The observed electron accumulation at the surface of n -type InN is due to the presence of positively charged donor-type surface states. The existence of such surface states requires that the following conditions are satisfied. First, in order to have predominantly donor-type character, the surface states must lie below the branch-point energy E_B . This is the crossover point from states higher in the gap that are mainly of conduction band character (acceptor-type) to states lower in energy that are mainly of valence band character (donor-type) [19,20]. This

branch-point energy falls close to the center of the band gap (in one dimension) in the complex band structure [21]. Second, the surface states must be at least partly above the Fermi level, since valence band (donor-type) states are positively charged when unoccupied and neutral when occupied. The surface Fermi level can be pinned above the Γ -point conduction band minimum (CBM) by unoccupied, positively charged donor-type surface states. These donors acquire a positive surface charge by emitting electrons into the conduction band. This results in downward band bending and electron accumulation. This combined requirement that the surface states are ionized donors and lie above the Fermi level can be achieved only in n -type semiconductors when the Γ -point CBM lies significantly below E_B . For the Γ -point CBM to lie below the average midgap energy of the entire Brillouin zone, it must be particularly low in energy relative to the rest of the conduction band. The wurtzite InN band structure calculated using density functional theory (DFT) within the local density approximation (LDA) with quasiparticle (QP) corrections by Bechstedt *et al.* [22] indicates that the Γ -point CBM is indeed much lower than the overall conduction band. Moreover, the results of these calculations also provide information from which the branch-point energy of InN can be estimated. This allows the existence of ionized donor-type surface states to be explained, to a first approximation, in terms of the bulk band structure.

Since the Γ -point conduction band energy bears little relation to the conduction band edge as a whole, Tersoff's approximate, semiempirical method for obtaining the branch-point energy of a semiconductor uses the indirect CBM and an effective VBM that takes account of the effect of spin-orbit splitting [21]. Using the indirect CBM at the A point of the QP-corrected DFT-LDA InN band structure [22] locates the branch-point energy E_B at 1.80 eV above the VBM and $\sim 1.05 \text{ eV}$ above the Γ -point CBM. To achieve overall charge neutrality, the Fermi level at the surface is expected to lie in the vicinity of this branch-point energy. As shown in Fig. 4, the surface Fermi level was found, from the charge-profile calculations, to be $\sim 1.64 \text{ eV}$ above the VBM and therefore close to E_B . For the donor-type surface states to be charged, and thus explain the observed electron accumulation, they must be at least partially unoccupied and therefore lie above the Fermi level. Details of the structure and chemistry of the surface are also important in determining the exact position of the surface Fermi level, but their importance is secondary to that of the bulk band structure. The phenomenon of a low Γ -point CBM also explains the electron accumulation that occurs at clean InAs surfaces [7]. The Γ -point CBM in III-V semiconductors is sensitive to the cation and decreases rapidly for a particular anion with increasing atomic number. For the other In-containing III-Vs, InP and InSb, the anion's influence on the valence bands pulls the branch point down in energy

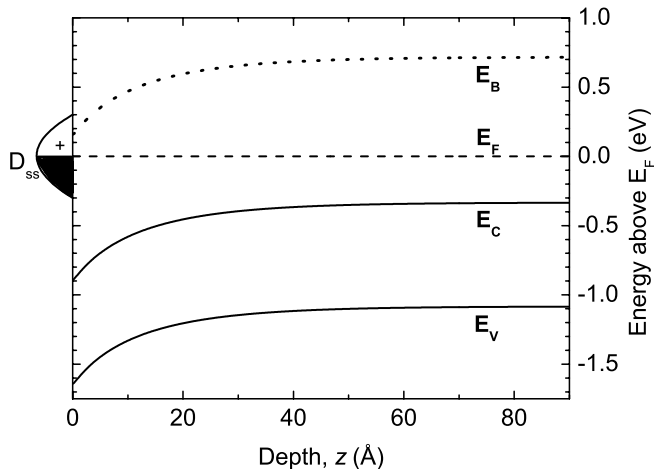


FIG. 4. The conduction and valence band edges (E_C and E_V , solid lines) and the branch-point energy (E_B , dotted line) with respect to the Fermi level (E_F , dashed line) in the near-surface region of InN(0001). The donor-type surface states (D_{ss}) are also shown, where the unoccupied states above the Fermi level are shown to be positively charged.

to below the Γ -point CBM, preventing them from exhibiting charge accumulation at their clean surfaces [21].

Electron-energy-loss spectroscopy of conduction band plasmon excitations reveals the existence of intrinsic charge accumulation at the clean InN(0001) surface. Charge-profile calculations reveal a surface state density of $\sim 2.5 \times 10^{13} \text{ cm}^{-2}$, which gives rise to a band bending of 0.56 eV to maintain charge neutrality, thus locating the Fermi level 1.64 eV above the VBM at the surface. The electron accumulation is a consequence of ionized donor-type surface states pinning the surface Fermi level high above the conduction band minimum. The surface Fermi level is not anomalously high in the overall band structure, but rather the Γ -point CBM is unusually low relative to the rest of the conduction band edge.

*Electronic address: C.F.McConville@warwick.ac.uk

- [1] J. Wu, W. Walukiewicz, K. M. Yu, J.W. Ager III, E. E. Haller, H. Lu, W. J. Schaff, Y. Saito, and Y. Nanishi, *Appl. Phys. Lett.* **80**, 3967 (2002).

- [2] J. Wu, W. Walukiewicz, K. M. Yu, J.W. Ager III, E. E. Haller, H. Lu, and W. J. Schaff, *Appl. Phys. Lett.* **80**, 4741 (2002).
- [3] H. Lu, W. J. Schaff, L. F. Eastman, and C. E. Stutz, *Appl. Phys. Lett.* **82**, 1736 (2003).
- [4] K. A. Rickert, A. B. Ellis, F. J. Himpsel, H. Lu, W. J. Schaff, J. M. Redwing, F. Dwikusuma, and T. F. Kuech, *Appl. Phys. Lett.* **82**, 3254 (2003).
- [5] T. D. Veal and C. F. McConville, *Phys. Rev. B* **64**, 085311 (2001).
- [6] H. Ibach and D. L. Mills, *Electron Energy-Loss Spectroscopy and Surface Vibrations* (Academic, New York, 1982).
- [7] M. Noguchi, K. Hirakawa, and T. Ikoma, *Phys. Rev. Lett.* **82**, 2243 (1991).
- [8] H. Lu, W. J. Schaff, J. Hwang, H. Wu, W. Yeo, A. Pharkya, and L. F. Eastman, *Appl. Phys. Lett.* **77**, 2548 (2000).
- [9] T. D. Veal, M. J. Lowe, and C. F. McConville, *Surf. Sci.* **499**, 251 (2002).
- [10] R. Fuchs and K. L. Kliewer, *Phys. Rev.* **140**, A2076 (1965).
- [11] Ph. Lambin, J. P. Vigneron, and A. A. Lucas, *Phys. Rev. B* **32**, 8203 (1985).
- [12] J. Wu, W. Walukiewicz, W. Shan, K. M. Yu, J.W. Ager III, E. E. Haller, H. Lu, and W. J. Schaff, *Phys. Rev. B* **66**, 201403 (2002).
- [13] A. Kasic, M. Schubert, Y. Saito, Y. Nanishi, and G. Wagner, *Phys. Rev. B* **65**, 115206 (2002).
- [14] E. O. Kane, *J. Phys. Chem. Solids* **1**, 249 (1957).
- [15] K. F. Berggren and B. E. Sernelius, *Phys. Rev. B* **24**, 1971 (1981).
- [16] I. Mahboob, T. D. Veal, and C. F. McConville, *Appl. Phys. Lett.* **83**, 2169 (2003).
- [17] M. J. Lowe, T. D. Veal, A. P. Mowbray, and C. F. McConville, *Surf. Sci.* **544**, 320 (2003).
- [18] H. Ubensee, G. Paasch, J. P. Zollner, and S. Handschack, *Phys. Status Solidi B* **147**, 823 (1988).
- [19] H. Luth, *Surfaces and Interfaces of Solid Materials* (Springer, Berlin, 1995).
- [20] W. Monch, *Semiconductor Surfaces and Interfaces* (Springer, Berlin, 1993).
- [21] J. Tersoff, *Phys. Rev. B* **32**, 6968 (1985).
- [22] F. Bechstedt, J. Furthmuller, M. Ferhat, L. K. Teles, L. M. R. Scolfaro, J. R. Leite, V. Y. Davydov, O. Ambacher, and R. Goldhahn, *Phys. Status Solidi A* **195**, 628 (2003).